LA-UR -85-1792

RECEIVED BY OSTI JUN 07 1985

CONF-8505100--7

LA-UR--85-1792

DE85 012739

TITLE: DETERMINATION OF CTX EQUILIBRIA

AUTHOR(S). S(tephen) O. Knox, Cris W. Barnes, CTR-5
G(eorge) J. Marklin, CTR-6; T(homas) R. Jarboe, CTR-5
I(vars) Henins, H(iroshi) W. Hoida, B(radford) L. Wright, CTR-5

SUBMITTED TO. 7th Symposium on Compact Toroid Research
Santa Fe, NM May 21-24, 1985

DISCLAIMER

Los Alamos Los Alamos National Laboratory
Los Alamos, New Mexico 87545

FORM NO 836 R4
ST NO 2629 5/81

DETERMINATION OF CTX EQUILIBRIA

S. O. Knox, Cris W. Barnes, G. J. Marklin, T. R. Jarboe
I. Henins, H. W. Hoida and B. L. Wright
Los Alamos National Laboratory, Los Alamos, New Mexico 87545

ABSTRACT

The method by which we determine the magnetic field equilibrium for CTX in a nonperturbing manner is presented. Measurements of flux conserver image currents are combined with calculations from a numerical model of the equilibrium. Results give equilibria which differ significantly from the miniumum energy state, but the equilibria data are well-described by a model where j/B has a linear dependence on the poloidal flux function. The observation of non-disruptive rotating internal kink distortions (with toroidal mode numbers n = 1,2 and 3) within the equilibria and theoretical MHD thresholds for the onset of these modes corroborate the inferred equilibria.

The magnetic fields of a spheromak are conjectured[1] to relax towards a state of minimum energy subject to the constraint that the magnetic helicity is conserved. The equation for this equilibrium in a closed system is $\nabla \times \underset{\sim}{B} = \lambda \underset{\sim}{B}$ with $\lambda = \mu_o j/B$ = constant. Since competing effects are certainly present in any experiment, λ is not expected to be uniform and constant throughout the duration of the discharge. However, departures from the minimum energy or "Taylor" state are expected[1] to relax towards this lowest energy configuration.

Previous experiments have measured the spheromak magnetic fields with internal probes. Turner, et. al.[2] found good agreement with a zero pressure, constant λ model, whereas Hart,et. al.[3] obtained better agreement with their data by including a finite pressure correction to a constant λ model. We report results which give spheromak equilibria not in the minimum energy state, but having $\lambda = \lambda(\psi)$, where ψ is the normalized poloidal flux function (ψ = poloidal flux value/total poloidal flux). The equilibria are observed not to relax back to the minimum energy state (constant λ) as the configuration resistively decays. Rotating kink modes within the equilibrium generate coherent oscillations (saturated in amplitude) in the surface current signals. These internal kink distortions have toroidal mode numbers n = 1,2 and 3 at different phases of the discharge. The onset of the modes is shown to be associated with the slope of $\lambda(\psi)$.

The $\lambda(\psi)$ profile is inferred from measurements of image currents flowing in a mesh flux conserver[4] (MFC) surrounding the plasma combined with results from numerical calculations of the equilibrium. This general technique has been used before to establish the MHD equilibrium in non-circular cross-section tokamaks [see Ref. 5 and references therein]. Arrays of small Rogowski loops are used to measure the induced image currents in the MFC. Each loop is wound on a 0.35 cm diameter dielectric rod 10 cm long, machined to ensure a high degree of uniformity between loops. The vacuum jacket of each loop is a 0.48 cm tantalum tube closed on one end with the other end joined to a 0.3 cm diameter stainless steel tube to exit the vacuum chamber. Individual coil assemblies are bent around the appropriate flux conserver rod to form the Rogowski loops. The loops (17 are used in the equilibrium measurement) have less than a 5% standard deviation in their relative calibration. Only the ratios of toroidal currents (filtered to remove oscillations) at different poloidal angles are used in the determination of the spheromak equilibrium. The present MFC, similar to but larger than the one outlined in Ref. 5, is approximately an oblate spheroid of diameter 136 cm

and length 62 cm. It is constructed of 1.3 cm diameter OFHC copper rods welded together at the rod crossings to form a mesh with a nominal spacing of 5 cm.

An axisymmetric ideal MHD equilibrium is computed by solving the Grad-Shafranov equation, with the $\lambda(\psi)$ profile and the boundary conditions specified[6]. The plasma pressure is assumed to be zero and $\lambda(\psi)$ is approximated by the linear function $\lambda(\psi)=\bar{\lambda}[1+\alpha(2\psi-1)]$, with the free parameter α to adjust the slope. The coefficient $\bar{\lambda}$ is the average of $\lambda(\psi)$ over ψ and is determined by the geometry and α. Each toroidal hoop of the MFC is assumed to be a perfect flux conserver, containing no net flux. In the model, all plasma currents are confined to the interior of the MFC. Using these boundary conditions, the hoop image currents are then calculated as a function of α. The best fit to the measured image currents is obtained by varying the value of α. Once $\lambda(\psi)$ is known, the inverse rotational transform $q(\psi)$ is calculated.

This procedure can obviously be extended to include more free parameters in the functional dependence of λ on ψ, such as a curvature term in $\lambda(\psi)$ or a finite pressure effect. Inclusion of a finite plasma pressure in the numerical models does alter the MFC current distribution. But, for the Thomson-scattering-measured pressures of similar CTX discharges [$\langle\beta\rangle_{vol}$ of 3-5%], the effect is within the composite error of the present method. The dominate effect on the MFC currents is due to the zero-pressure $\lambda(\psi)$ profile. A linear $\lambda(\psi)$ functional dependence fits the data well.

The evolution of a typical CTX discharge has two phases: the formation and sustainment phase when magnetic helicity is injected to build-up and maintain the spheromak fields, and the resistive decay phase which begins when the helicity source is turned off. One representative discharge has been selected for detailed analysis here. The spheromak was formed by a magnetized coaxial plasma source operating with a square pulse (0.1 - 0.7 ms) source current waveform. The resulting spheromak toroidal plasma current is given in Fig. 1(a).

As the spheromak equilibrium changes from the sustainment to the decay phase, the magnetic axis moves radially outward, and the relative amount of toroidal current flowing in the MFC at different poloidal locations changes. Figure 1(b) shows examples of the time behavior of two MFC toroidal currents at the same toroidal angle but at different poloidal positions, one near the symmetry axis and one near the maximum radius of the flux conserver. (The oscillations apparent in Fig. 1(b) are discussed in Ref. 7.) Throughout formation and sustainment the ratio of the filtered currents remains nearly constant. After sustainment, the MFC toroidal currents near the symmetry axis decay more rapidly than the currents near the outside midplane.

Figure 2 is a summary of the time evolution of the equilibrium. The circles of Fig. 2(a) are the experimental values for the MFC toroidal hoop current ratios, and the solid lines are the theoretical current ratios for the two choices of α which bound the experimental data. Toroidal mode numbers for the oscillations occuring during the indicated time intervals are given in the figure. Using the values for α, the corresponding $\lambda(\psi)$ and $q(\psi)$ for the equilibria are then calculated. They are shown in Figs. 2(b) and (c), respectively. During the formation phase (.1-.7 ms), the $\lambda(\psi)$-profile [c.f. Fig. 2(b)] is peaked towards the outside of the configuration ($\psi \to 0$), indicating a relatively high value of j/B in that region. This is consistent with the interpretation of spheromak sustainment by currents driven primarily on the outer flux surfaces. The CTX experiment has maintained this non-minimum energy equilibrium during sustainment for up to 6 ms ($> 10\tau_{R0}$). In the next time interval (0.8-1.05 ms), no oscillations are present and the

$\lambda(\psi)$-profile is essentially independent of ψ. This is the only time when the equilibrium is near the minimum energy or Taylor state. The spheromak does not remain in this state, nor does it return during the remainder of the resistive decay phase of the plasma. During the following time interval (1.1-1.3 ms), the $\lambda(\psi)$-profile changes slope with resistivity gradients causing j/B to peak towards the magnetic axis ($\psi \to 1$), resulting in a drop in q. The peaking continues during the next time interval (1.45-1.55 ms), where the $\lambda(\psi)$ slope increases even further. The configuration then terminates in this discharge, when the particle density goes to zero.

A convienent method for visualizing the evolution of the equilibrium via the linear $\lambda(\psi)$ profile is to plot the slope parameter α versus time, as shown in Fig. 3. The shaded band is the $\alpha(t)$ (plus error) for discharges which develop an n = 3 mode, and the cross-hatched area is for a set of discharges with higher plasma density which develop only an n = 2 mode in the decay phase. The trend of Fig. 3 is evident: for the former case (shaded), $\alpha \simeq -.3$ for the sustainment phase, passes through zero (minimum energy state), and then continues to increase for the remainder of the discharge. However, the $\alpha(t)$ trajectory for discharges with only n = 2 modes is different, as the $\alpha(t)$ trajectory rolls over at $\alpha \simeq .5$. Consequently, the $\lambda(\psi)$ slope does not continue to increase as rapidly in time. The transport properties of these discharges (formed at higher filling pressure[8]) reduce the rate at which j/B continues to to peak towards the magnetic axis, and the spheromaks do not become n = 3 unstable. Discharges with only n = 2 modes have, in general, longer decay phases (up to 1.9 ms) than those with n = 3 modes.

The α-parameter is also used to compare estimates from a linear ideal MHD stability analysis (detailed in Ref. 9) with the occurence of the observed unstable modes. The growth rate γ_n for the fastest growing toroidal mode number n is determined as a function of α and hence the equilibrium. The square of this growth rate is plotted in Fig. 4 for the n = 1,2,3 and 4 modes. It is normalized to the Alfven transit time $\tau_A = R/\langle V_A \rangle$, where $\langle V_A \rangle = (\int B^2 dv/\mu_o \int \rho dv)^{1/2}$ is the volume-averaged Alfven speed. Figure 4 shows the n = 2 mode becoming unstable when α is .25 and the $q(\psi)$ at the magnetic axis, q_a, is approximately 1/2. The n = 3 mode takes over when $\alpha \simeq .7$ and $q_a \simeq 1/3$. These values of α agree well with the appearance of the n = 2 and n = 3 modes in the experiment (see Figs. 2 and 3). The n = 1 ideal MHD mode however, does not become unstable until $\alpha \simeq -.5$ and q_a is substantially above 1. The observed n = 1 mode, which appears when $\alpha \simeq -.3$ and $q_a \simeq 1$, is probably the result of a resistive instability with a lower threshold.

In summary, a method for determining experimental spheromak equilibria by combining measurements of flux conserver image currents with numerical modeling techniques has been presented. Because of nonuniform resistivity, spheromak equilibria are observed to maintain departures from minimum energy profiles for times greater than the resistive decay time of the configuration, and are found to be near the minimum energy state for only a short time during the discharge. Deviations from the minimum energy state in a low-β spheromak apparently do not require a concomitant relaxation. The nondisruptive internal kink modes present in these equilibria have toroidal mode numbers (n = 1,2, and 3 at different times during the discharge) associated with the slope of the $\lambda(\psi)$-profile. These modes occur at times during the discharge which substantiate the inferred equilibria.

This work is supported by the U. S. Department of Energy.

REFERENCES

[1] J. B. Taylor, Phys. Rev. Lett. 33, 1139 (1974).

[2] W. C. Turner, G. C. Goldenbaum, E. H. A. Granneman, J. H. Hammer, C. W. Hartman, D. S. Prono, and J. Taska, Phys. Fluids 26, 1965 (1983).

[3] G. W. Hart, C. Chin-Fatt, A. W. DeSilva, G. C. Goldenbaum, R. Hess, and R. S. Shaw, Phys. Rev. Lett. 51, 1558 (1983).

[4] T. R. Jarboe, Cris W. Barnes, I. Henins, H. W. Hoida, S. O. Knox, R. K. Linford, and A. R. Sherwood, Phys. Fluids 27, 13 (1984).

[5] J. L. Luxon and B. B. Brown, Nucl. Fusion 22, 813 (1982).

[6] G. Marklin, U. S. - Japan Workshop on Compact Toroids, Japan (1984).

[7] B. L. Wright, in Proceedings Sixth Symposium on Compact Toroid Research, p. 5, Princeton (1984); also T. R. Jarboe, et. al., in Plasma Physics and Controlled Nuclear Fusion Research, London, 1984 (IAEA, Vienna) to be published.

[8] C. W. Barnes, T. R. Jarboe, I. Henins, A. R. Sherwood, S. O. Knox, et. al., Nucl. Fusion 24, 267 (1984).

[9] G. Marklin, in Proceedings Sixth Symposium on Compact Toroid Research, p. 88, Princeton (1984).

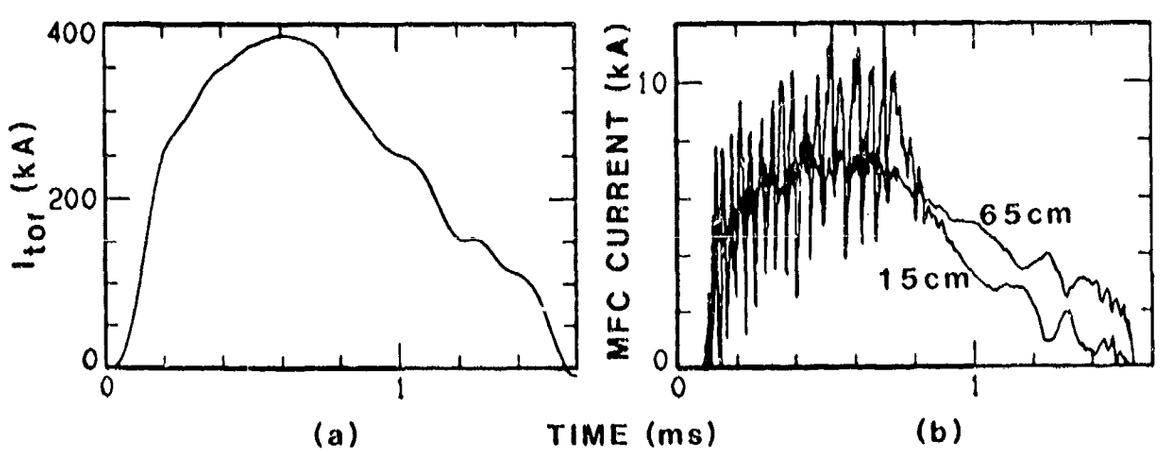

Figure 1. (a) Total torodial plasma current. (b) Examples of MFC torodial hoop currents. Distances given are the radii from the symmetry axis for the Rogowski loops.

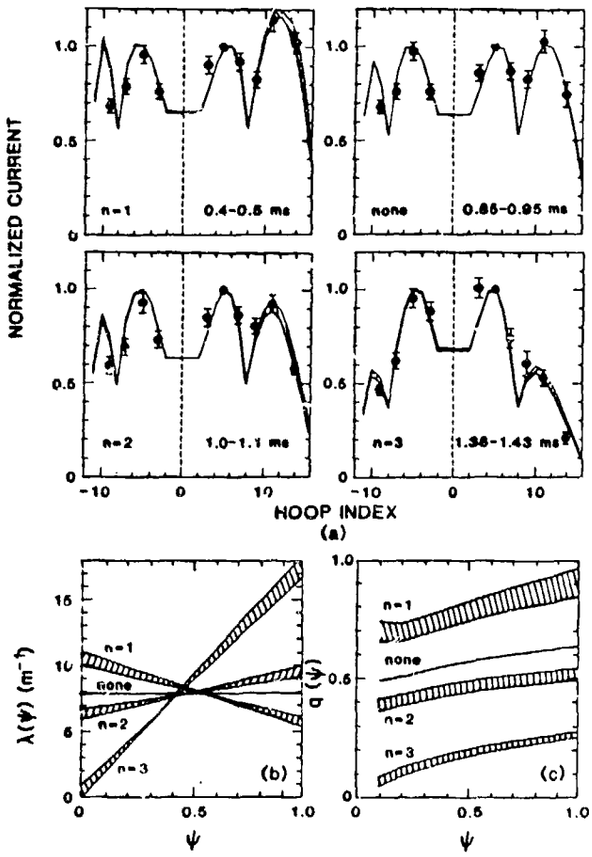

Figure 2. Time evolution of the equilibrium. (a) Experimental values (circles - normalized to hoop 5) and theoretical MFC toroidal hoop current ratios (solid lines) for the indicated averaging times. The sharp minima in the theoretical curves correspond to the corners of the MFC, and the vertical dotted line is the MFC midplane. Values of α for the indicated time intervals are: $\alpha = -.35$ and $-.25$; $\alpha = 0$; $\alpha = .15$ and $.25$; $\alpha = .9$ and 1.0. The hoop index runs from -11 (entrance region) to +16 (symmetry axis). (b) $\lambda(\psi)$ vs. ψ profiles for (a). (c) $q(\psi)$ vs. ψ profiles for (a).

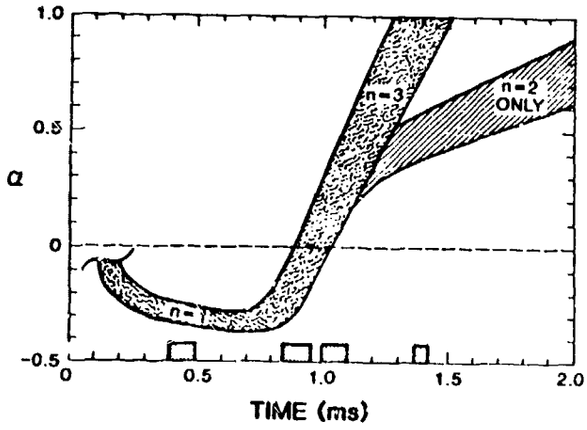

Figure 3. Experimental trajectory of the $\lambda(\psi)$ slope parameter α vs. time. Times indicated at the bottom correspond to the equilibria of Fig. 2.

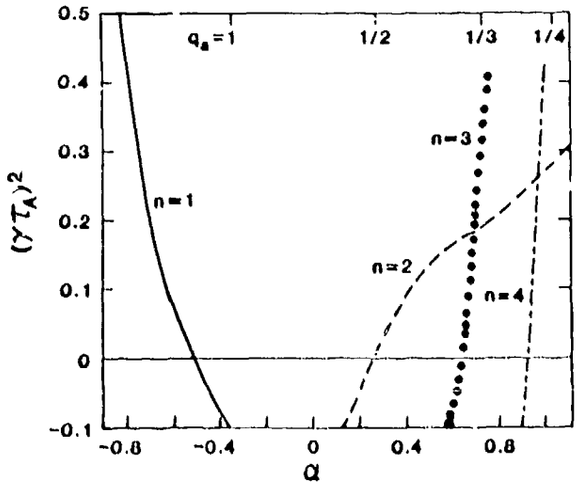

Figure 4. Square of the normalized toroidal mode growth rate vs. α from linear ideal MHD stability analysis. The value of q_a is given at the top of the figure.